

Multiple Doping (Ag+Fe+La) Induced Altering of the Magnetic and Antibacterial Properties of ZnO Nano Powders

Sathish P*

Department of Physics, Arts and Science College, Bharathidasan University, Thanjavur, Tamil Nadu-613007, India

Abstract

In the current scenario, undoped, Ag (2 at. %), Ag + Fe (2 at. %) and Ag + Fe+ La (2 at. %) doped ZnO Nano powders were fabricated using combustion method and their basic properties were characterized. The doped samples exhibit better ferromagnetic behavior in the case of magnetic studies. The grain size of the pristine ZnO is around 200 nm and the size reduces drastically at one order of magnitude (from 200 nm to 22 nm) after doping in the surface morphological studies. The gradual decrease in the crystallite size is significantly due to the zener pinning effect as confirmed by structural studies. The antibacterial efficiency of the synthesized samples is examined against three different bacteria specifically *Staphylococcus aureus*, *Bacillus subtilis* (Gram Positive) and *Shigella flexneri* (Gram Negative), testified that the antibacterial efficacy of ZnO sample increases rapidly after doping. As a consequence, the doped and undoped ZnO Nano powders exhibit better efficiency against *S. flexneri* than *S. aureus* and *B. subtilis*. The optical quality of the semiconductor material is reported by photoluminescence (PL) studies.

Keywords: ZnO: Ag: Fe: La Nano powders; Combustion; HR-SEM; HR-TEM; Antibacterial activities

Corresponding author: Sathish P

✉ apsathish.physics@gmail.com

Post Graduate & Research Scholar,
Department of Physics, Annai Vailankanni
Arts and Science College, Thanjavur, Tamil
Nadu-613007, India.

Citation: Sathish P (2021) Multiple Doping (Ag+Fe+La) Induced Altering of the Magnetic and Antibacterial Properties of ZnO Nano Powders. Nano Res Appl Vol.7 No.3:8

Received: December 17, 2020; **Accepted:** March 20, 2021; **Published:** March 27, 2021

Introduction

Inorganic metal oxides have captivated the heed of the researchers as a consequence of their prospective applications in diverse fields and also immensely used in bio-medicalization [1]. There are various metal oxides transpires in nature, among those, zinc oxide, is a propitious material because of its unique property and also bio-compatible in nature [2-4]. In the food packaging materials, ZnO Nano powders play a pivotal role in controlling the harmful food borne bacteria [5]. Comparably, the adroit antibacterial activity of Ag and La, instantaneously the magnetic properties of Fe are optimistic, when the physical parameters exhibit Nano scale [6,7]. The carrier concentration is increased by a transition metal doping, leads to an enhanced antibacterial activity. Furthermore, metallic elements (Ag, Fe) and rare earth element (La) have been used as dopants in the existing work. In the current work, undoped, Ag, Fe and La doped ZnO Nano powders are synthesized and their structural, magnetic and antibacterial properties are characterized and reported.

Numerous methods are recruited for the synthesis of doped and

undoped ZnO Nano powders such as ultrasonic spray pyrolysis, sol-gel, precipitation, heteropolyometalates, soft chemical and combustion [8-13]. Among those methods, combustion method is extensively used because of the better yield as well as inexpensive.

Materials and Methods

Synthesis process

The starting solution is taken in the quantity of (0.2 M) by dissolving the host precursor zinc nitrate hex hydrate $[Zn(NO_3)_2 \cdot 6H_2O]$ in 200 ml of de-ionized water. Silver nitrate $[AgNO_3]$, ferric nitrate $[Fe(NO_3)_3]$ and Lanthanum nitrate hex hydrate $[La(NO_3)_3 \cdot 6H_2O]$ are used as dopant precursors for Ag, Fe and La, respectively. Undoped and Ag, Fe, La doped ZnO Nano powders are synthesized by adding adequate doping level (Ag- 2 at.%, Fe- 2 at.% and La- 2 at.%) in the initial solution. The pH value of the starting solution is maintained at 9, by adding desired amount of ammonia solution. To achieve the homogeneity in the final product, polyethylene glycol is added as surfactant which can be

used to acquire the gel formation. The existing mixture is heated at 70°C and magnetically stirred for 30 min. The mixture is shifted to heating mantle, after the completion of the stirring process, which is maintained at 95°C for 2 h till the mixture gets sparked. The calcination of the synthesized powder is maintained at 550°C for 2 h and authorized to achieve room temperature to procure the final product.

Microstructure characterization of ZnO: Ag: Fe: La Nano powders

The crystalline quality of the doped and undoped ZnO was measured using x-ray powder diffraction technique (Analytical-PW 340/60 X' pert PRO) using Cu-K_α radiation ($\lambda = 1.5406 \text{ \AA}$). Photoluminescence (PL) spectra were analyzed using spectrofluorometer (JobinYvon_FLUROLOG-FL3-11) with xenon lamp (450 W) as the excitation source, of wavelength 325 nm. Fourier transform infrared (FTIR) spectra were observed using Perkin Elmer RX-I FTIR spectrophotometer. The surface morphologies were recorded using high resolution scanning electron microscope [HRSEM] (FEI-Quanta FEG 200 F) and the high resolution transmission electron microscope [HRTEM] (JEOL JEM 2100). The elemental qualitative analysis was characterized using energy dispersive X-ray analysis (EDAX)

Estimation of antibacterial activity

The antibacterial activity of the undoped and doped ZnO Nano powders was tested against three different bacteria *viz.* *Staphylococcus aureus*, *Bacillus subtilis* (Gram Positive) and *Shigella flexneri* (Gram Negative) using well diffusion method. The influence of bacteria is rapid under the nutrient agar, which was used as medium. This agar medium was sterilized in an autoclave at 121°C for 15 minutes and then scattered across the petriplate. The UV laminar air flow chamber is used to attain solidification. Following the above process, a fresh bacterial culture was disseminating the plate using spread plate technique.

Each well of the petriplates was maintained at 5 mm in diameter using, sterile cork borer. All the wells of different bacteria were immunized with constant value of 100 $\mu\text{g/mL}$ in the final product of stock solution. The petriplates were incubated at 37°C for 24 h, following the above process the petriplates were adhered for the formation of clear zone of inhibition (ZOI) around the well. The antibacterial efficacy was recorded by measuring the diameter of the ZOI around the wells.

Results and Discussion

Structural studies

The XRD patterns of undoped, Ag, Ag+Fe and Ag+Fe+La doped ZnO Nano powders are shown in **Figure 1**. The diffraction peaks are well adapted with the JCPDS card no. 36-1451 of ZnO, confirms the hexagonal wurtzite structure. The existing planes, such as (100), (002), (101), (102), (110), (103), (201), and (202) are associated with polycrystalline ZnO.

Furthermore, the region with a diminished intensity is acquired for the doped ZnO Nano powders, due to the incorporation of dopants into the ZnO matrix. The plane (111) belongs to

the unmatched diffraction peak at $2\theta = 38.065^\circ$, signifying the presence of the secondary phase of metallic Ag.

The predominance of (101) peak is unchanged by the dopants Ag, Fe and La. The shift in the diffraction angles is not witnessed after doping, due to the formation of Ag as a separate phase. Besides, the ionic radii of Fe³⁺ (0.64 nm) and La³⁺ (0.115 nm) are comparable to their host counterparts Zn²⁺ (0.74 nm) and O²⁻ (0.132 nm) [14,15].

The crystallite size (D) of undoped and doped ZnO Nano powders is calculated using the Debye-Scherer's formula [16].

$$D = 0.9\lambda / \beta \cos\theta \quad (1)$$

Where λ (1.5406 \AA) is the wavelength of the X-ray used, β is the full width at half of its maximum intensity (FWHM) and θ is the Bragg's angle.

The lattice constants 'a' & 'c' and volume of the unit cell (V) are studied using the following formulae [17].

$$\frac{1}{d^2} = \frac{4}{3} \frac{(h^2 + hk + k^2)}{a^2} + \frac{l^2}{c^2} \quad (2)$$

$$V = \frac{\sqrt{3}}{2} a^2 c \quad (3)$$

The structural parameters are given in the **Table 1**. The undoped ZnO, exhibit the crystallite size of 32 nm. Moreover in the case of doped samples, the crystallite size decreases drastically, at the range of 27 nm, 23 nm and 18 nm. Meanwhile, in the case of Ag (2 at. %) doped ZnO; it generates more number of oxygen vacancies into the ZnO lattice. As a result, the growth of crystallites is restricted by the oxygen vacancies and also by the crystal defects like vacancies and interstitials, results in the zener pinning effect [18]. Additionally, the doping effect of Fe (2 at. %) and La (2 at. %) into the ZnO along with Ag, exhibit reduction in grain size, may be due to the negligible disparity in the ionic radii of the host and

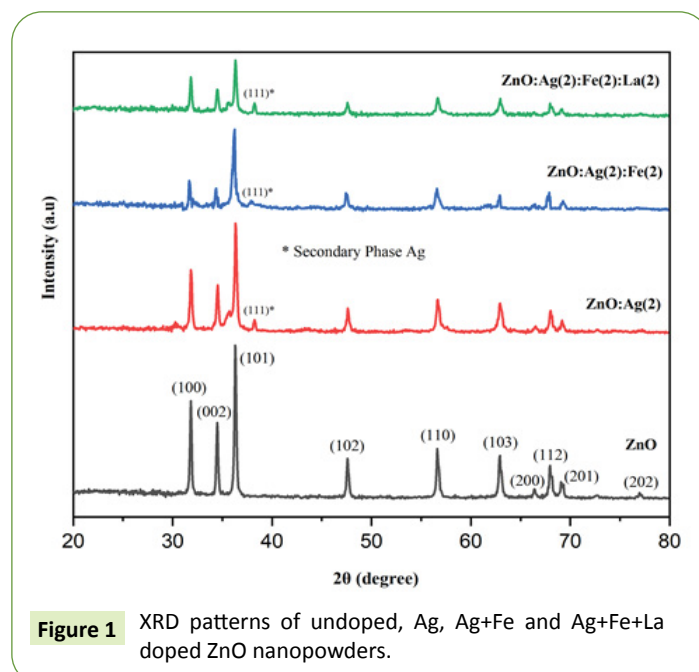


Figure 1 XRD patterns of undoped, Ag, Ag+Fe and Ag+Fe+La doped ZnO nanopowders.

Table 1 Structural parameters of ZnO: Ag: Fe: La Nano powders.

Doping Level (at %)	Lattice constants (Å)		D (nm)	V (Å) ³
	a	c		
ZnO	3.246	5.202	32	47.56
ZnO: Ag (2)	3.244	5.200	27	47.54
ZnO: Ag (2): Fe (2)	3.242	5.198	23	47.50
ZnO: Ag (2): Fe (2): La (2)	3.240	5.196	18	47.46

D- Crystallite size; V- Volume of the unit cell;
Standard values: a= 3.2498 Å, c = 5.2066 Å (JCPDS card no. 36-1451)

dopant ions. This causes a slight decrease in the value of lattice parameters.

FTIR studies

The FTIR spectra were measured in the range of 400–4000 cm⁻¹ to examine the presence of functional groups in the synthesized samples as shown in **Figure 2**. The Zn–O stretching vibration is attributed to the band appears approximately at 448 cm⁻¹ [19]. The band centered at around 424 cm⁻¹ is related to metal-oxygen stretching frequency band, owing to the presence of La-Zn-O. The peak emerges at around 2927 cm⁻¹ is related to the C-H bonding. Asymmetric and symmetric stretching modes of C=O are well fitted with the peaks at 1387 cm⁻¹ and 1586 cm⁻¹ [20]. The spot at 897 cm⁻¹ indicates the O-O bonding. The region around 3397 cm⁻¹ is the absorption band, confirms the hydroxyl stretching vibration (O-H), due to the occurrence of moisture content in the synthesized samples [21]. This hydroxyl group plays a vital role in the generation of hydroxyl radicals, results in the enhancement of antibacterial activity of the synthesized product as discussed, broadly in sec. 3.6.

Photoluminescence studies

The photoluminescence (PL) spectroscopy, displays the optical property, as well as their level of defects and impurity. The spectra at the excitation wavelength of 325 nm along with prominent peaks centered around 387 nm, 406 nm, 423 nm and 467 nm of undoped and doped ZnO Nano powders are shown in **Figure 3**. The peak found at 387 nm confirms the presence of near band edge (NBE) emission which emerges due to the band to band transition [22]. The region at 406 nm shows Ag in the doped cases, results in the change of electronic structure induced by the strain [23]. The significant factor for this strain is due to the ionic disparity between the dopant (Ag⁺= 0.126 nm) and host (Zn²⁺= 0.074 nm) ions.

The transition of electrons from zinc interstitials (Zn_i) to the valence band is closely associated with the strapping peak arises at 425 nm. The presence of singly ionized oxygen vacancies (V_o^+) is identified by the region 468 nm, causes the generation of OH⁻ ions which plays a crucial role in the antibacterial efficacy. The increase in the doping level of Fe exhibits a red shift owing to the *sp-d* exchange interactions [24]. The existence of more number of oxygen vacancies (v_o), may be caused by one of the dopants lanthanum [25].

Magnetic studies

The magnetic-hysteresis (M-H) curve demonstrates Zn surface spins, in the case of undoped ZnO leads to diamagnetic behavior

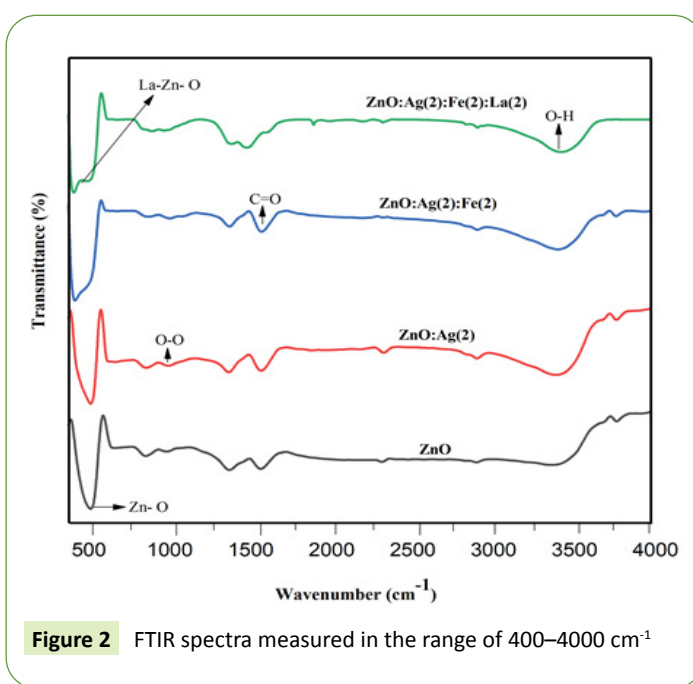


Figure 2 FTIR spectra measured in the range of 400–4000 cm⁻¹

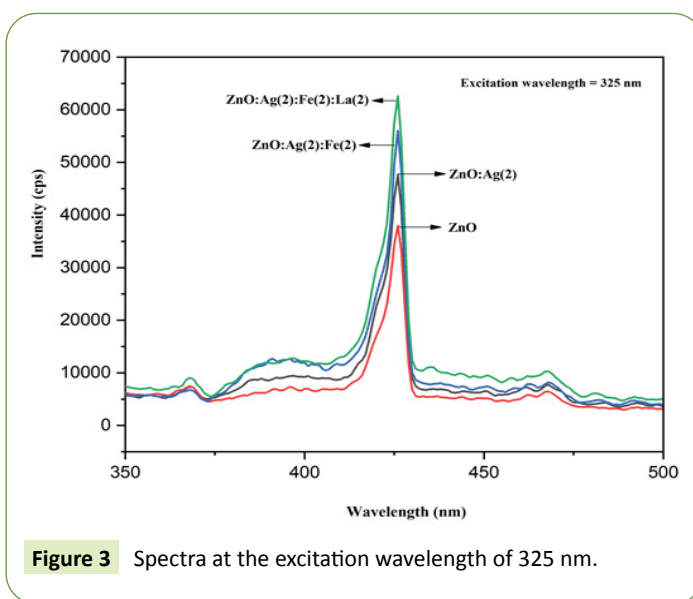


Figure 3 Spectra at the excitation wavelength of 325 nm.

as shown in **Figure 4** [26]. It is examined that the doped ZnO shows high saturation magnetization, due to the occurrence of more number of oxygen vacancies (v_o), effected by one of the dopants Ag. In the case of Ag (2 at. %) doped ZnO, it emits a slight ferromagnetic behavior at room temperature (RT-FM), due to the

occupancy of Ag atoms into ZnO lattice and causes the sight of bound magnetic polarons (BMPs) at a temperature of 300 K [27]. As a result, the oxygen vacancies (v_o) and the magnetic Ag ions create more number of magnetic polarons. Furthermore, Fe (2 at.%) and La (2 at.%) doped ZnO Nano powders along with Ag, shows a solid ferromagnetic behavior at room temperature (RT-FM), due to the oxidation states of Fe in mixed valency (Fe^{2+} and Fe^{3+}) [28]. The free electrons play a crucial role to connect all magnetic ions and the saturation magnetization value is inferior in the case of lanthanum doped ZnO (0.093 emu/g), comparing to Ag doped ZnO (0.09 emu/g), ascribed to the incorporation of La into the ZnO lattice and it can be extensively, used in spintronics and bio-medical applications.

HR-SEM, EDAX, and HR-TEM studies

HR-SEM and HR-TEM studies afford a broad report about the surface morphology and microstructures of the synthesized samples are shown in **Figure 5 (a-d)**. HR-SEM image, illustrates the undoped ZnO sample exhibits a loosely packed particles with irregular shape and size, approximately in the range of 150- 200 nm is shown in **Figure 5a** In the case of doped ZnO, the particle size decreases abruptly at one order of magnitude around ~ 32

nm, ~ 26 nm and ~22 nm is shown in **Figure 5 (b-d)**. As confirmed by the structural studies, zener pinning effect plays a crucial role in the rapid decrease of particle size. Consequently, there is an increase in the surface to volume ratio that supports to afford high contact area to the bacteria, results in the enhancement of antibacterial activity. As shown in figure the EDAX spectrum confirms the presence of the predictable elements Zn, O, Ag, Fe, La and the compositional mapping reveals the distribution of elements in a uniform manner throughout the surface (**Figure 6**). The examined grain sizes from the HR-TEM images are in good arrangement with HR-SEM results are shown in **Figure 7**.

Antibacterial activities

The antibacterial activity is tested against three different bacteria viz. *Staphylococcus aureus*, *Bacillus subtilis* (Gram Positive) and *Shigella flexneri* (Gram Negative) using agar well diffusion method is shown in **Figure 8**. The antibacterial efficacy was noted by measuring the diameter of the zone of inhibition (ZOI) around the wells and demonstrated, graphically as shown in **Figure 9**. From the zone of inhibition, it is observed that Ag (2 at.%), Fe (2 at.%) and La (2 at.%) doped ZnO samples illustrate the improved antibacterial efficiency against all three different bacteria. The

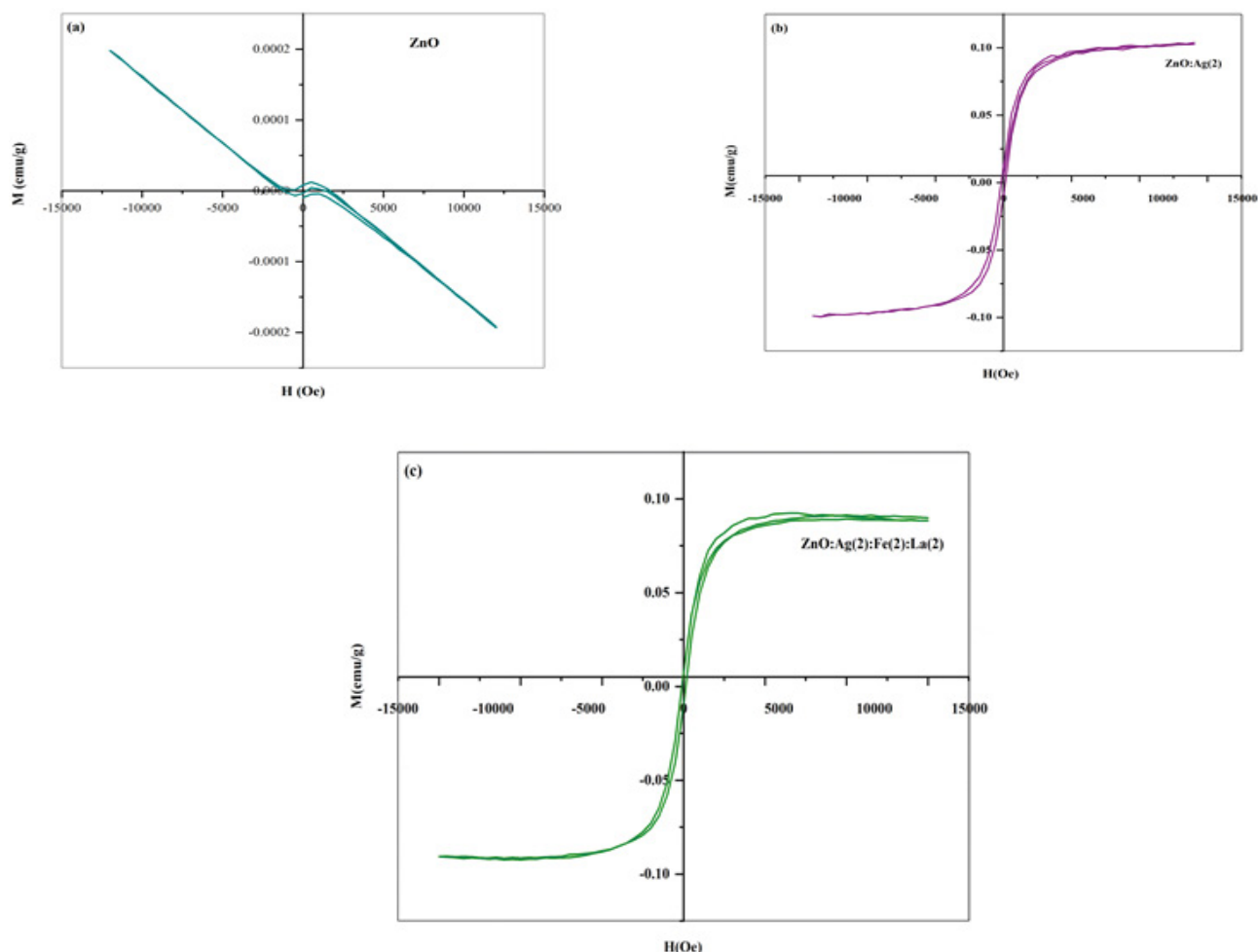


Figure 4 Magnetic-hysteresis (M-H) curve demonstrates Zn surface.

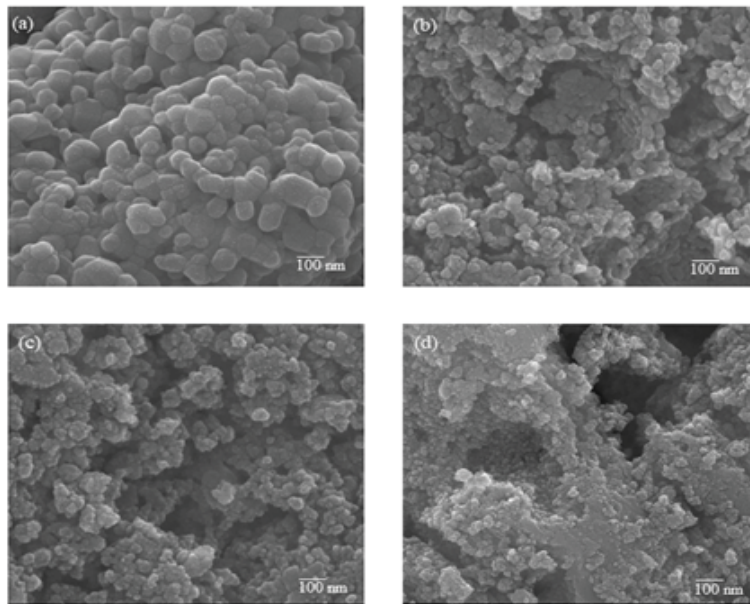
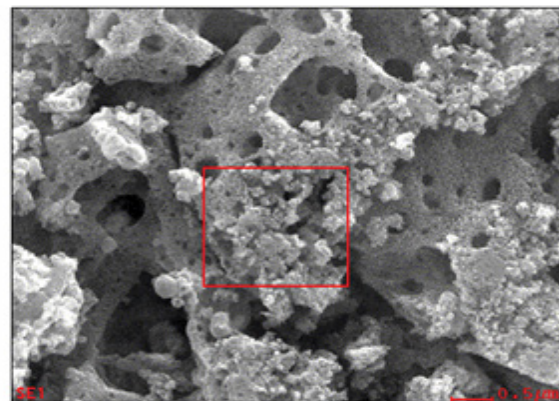
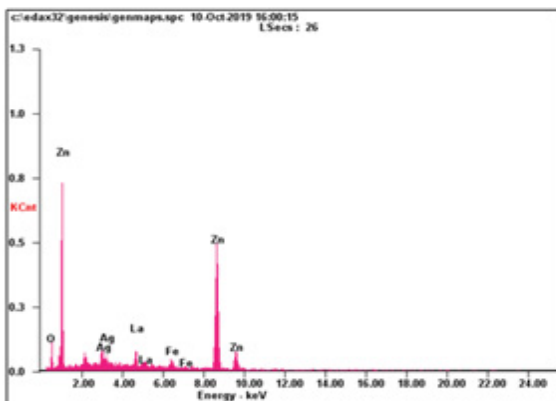


Figure 5 HR-SEM and HR-TEM studies afford a broad report about the surface morphology and microstructure of the synthesized.



Element	Wt%	At%
OK	14.46	42.60
AgL	06.16	02.02
LaL	07.02	02.01
FeK	02.40	01.99
ZnK	69.30	49.99

Figure 6 EDAX spectrum confirms the presence of the predictable elements Zn, O, Ag, Fe, La and the compositional mapping reveals the distribution of elements in a uniform manner throughout the surface.

significant factors responsible for the increase in the antibacterial efficiency are: (i) the reduction in particle size (ii) generation of reactive oxygen species (ROS).

Generally, Ag is considered as the robust germ-destroying agent. In the case of Ag (2 at.%) doped ZnO, the substitutional incorporation of Ag⁺ ions into the ZnO lattice, results in the

occupancy of interstitial position by Zn²⁺ ions as confirmed by PL studies [29]. The inclusion of Fe (2 at. %) as a second dopant, is to alter the magnetic property of the Ag doped ZnO. Fascinatingly, this Fe incorporation shows an improved antibacterial activity may be due to the substitution of Fe³⁺ ions into the Zn²⁺ sites. As a result, release of free electron occurs with respect to the

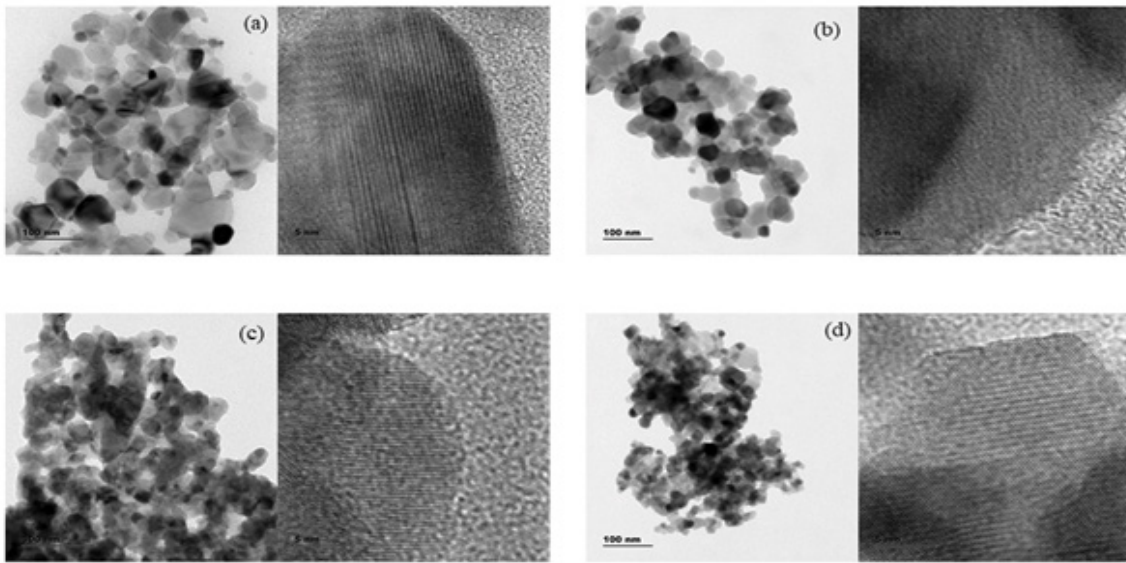


Figure 7 The examined grain sizes from the HR-TEM images are in good arrangement with HR-SEM results.

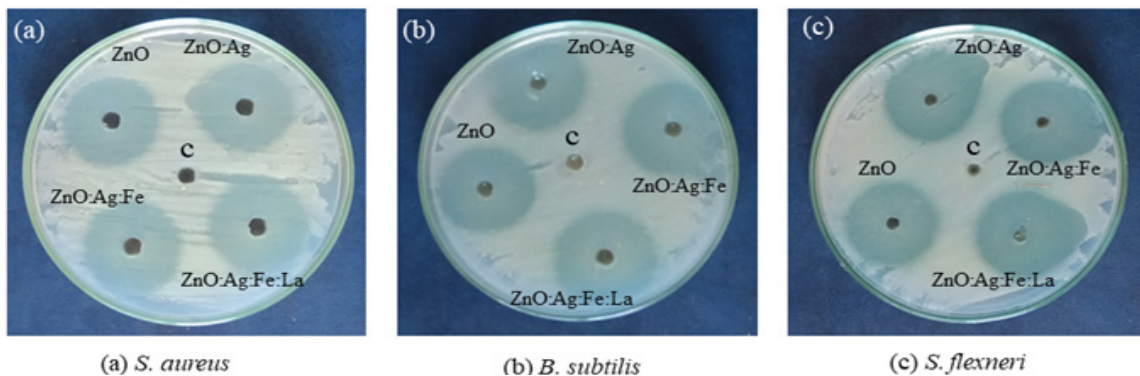


Figure 8 The antibacterial activity is tested against three different bacteria viz. *Staphylococcus aureus*, *Bacillus subtilis* (Gram Positive) and *Shigella flexneri* (Gram Negative) using agar well diffusion method.

substitution of each Fe^{3+} ion, leads to the generation of reactive oxygen species (ROS) viz. hydroxyl radicals, superoxide anion and hydrogen peroxide [H_2O_2]. The effect caused by hydroxyl radicals and superoxide anion, in the destruction of lipids, proteins and DNA of the bacteria, is mainly due to their negative charge. Moreover H_2O_2 plays a crucial role by penetrating directly into the cell membrane of the bacteria and destroys the growth of bacterial cell [30]. The effect of third dopant La (2 at. %), results in the release of heavy metal ions like La^{3+} and Zn^{2+} . The cell wall of the bacteria comprises of teichoic acid, which releases negative charge due to the presence of phosphate in their structure. The Zn^{2+} and La^{3+} ions possess positive charge, results in the penetration of metal ions inside the cell surface of bacteria. Among the three bacteria tested for antibacterial activity, *S. flexneri* (Gram Negative) bacteria shows enhanced efficiency compared with, *S. aureus* and *B. subtilis* (Gram Positive) bacteria, which may be due to the physical interruption of the cell membrane, owed to its low resistance [31].

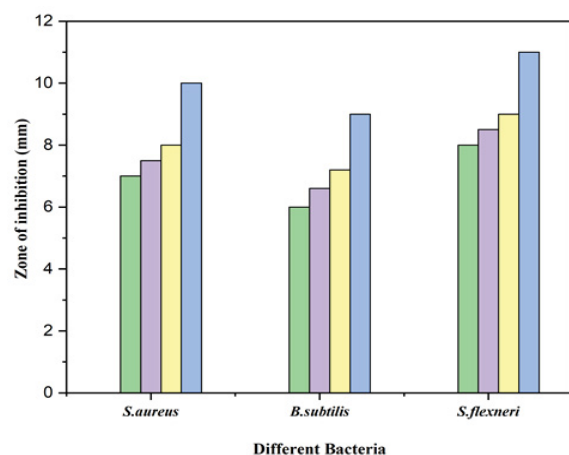


Figure 9 The antibacterial efficacy was noted by measuring the diameter of the zone of inhibition (ZOI) around the wells and demonstrated, graphically.

Conclusion

The doped (ZnO:Ag:Fe:La) Nano powders emit strong ferromagnetic behavior and displays better antibacterial efficiency compared to undoped ZnO sample is caused by the effect of dopants, in the existing work. Among the doped cases, Ag+Fe+La doped ZnO exhibits a better antibacterial efficacy against all the three tested bacteria viz *S. flexneri*, *S. aureus* and *B. subtilis*. The combined ferromagnetic and antibacterial properties of the

impurity added ZnO Nano powders are comprehensively used in spintronics and in the field of targeted drug delivery.

Acknowledgement

The author gratefully acknowledge the SAIF, IIT Madras, Tamil Nadu, India, for their timely manner and sincerely acknowledges, the Secretary & Correspondent, Administrator and Principal, Annai Vailankanni Arts and Science College, Thanjavur - 613 007, Tamil Nadu, India, for their encouragement and support.

References

- 1 Sadeghi B A study on the stability and green synthesis of silver nano particles using *Ziziphora tenuior*. (2014) *Spectrochim Acta A* 118-787.
- 2 Gonzalez-Hernandez R, Martinez AI, Falcony C, Lopez AA, Pech-Canul MI, et al. (2010) Study of the properties of undoped and fluorine doped zinc oxide nanoparticles. *Materials Letters*. 64: 1493-1495.
- 3 Lellouche J, Kahana E, Elias S, Gedanken A, Banin (2009) E. Antibiofilm activity of nanosized magnesium fluoride. *Biomaterials*. 30: 5969-5978.
- 4 Ramani M, Ponnusamy S, Muthamizhchelvan C, Cullen J, Krishnamurthy S, et al. (2013) Morphology-directed synthesis of ZnO nanostructures and their antibacterial activity. *Colloids and Surfaces B: Biointerfaces*. 105: 24-30.
- 5 Panea B, Ripoll G, González J, Fernández-Cuello Á, Albertí P (2014) Effect of nanocomposite packaging containing different proportions of ZnO and Ag on chicken breast meat quality. *J Food Eng* 123: 104-112.
- 6 Sharma N, Kumar J, Thakur S, Sharma S, Shrivastava V (2013) Antibacterial study of silver doped zinc oxide nanoparticles against *Staphylococcus aureus* and *Bacillus subtilis*. *Drug Invention Today*. 5: 50-54.
- 7 Jayanthi K, Chawla S (2010) Synthesis of Mn doped ZnO nanoparticles with biocompatible capping. *Appl Surf Sci* 256: 2630-2635.
- 8 Flores G, Carrillo J, Luna JA, Martínez R, Sierra-Fernández A, Milosevic O, (2014) Synthesis, characterization and photo catalytic properties of nanostructured ZnO particles obtained by low temperature air-assisted-USP. *Adv Powder Technol* 25: 1435-1441.
- 9 Zak AK, Majid WA, Mahmoudian MR, Darroudi M, Yousefi R (2013) Starch-stabilized synthesis of ZnO nanopowders at low temperature and optical properties study. *Adv Powder Technol* 24: 618-624.
- 10 Wang H, Li C, Zhao H, Liu J (2013) Preparation of Nano-sized flower-like ZnO bunches by a direct precipitation method. *Adv Powder Technol* 24: 599-604.
- 11 Rashidi H, Ahmadpour A, Bamoharram FF, Heravi MM, Ayati A (2103) The novel, one step and facile synthesis of ZnO nanoparticles using heteropolyoxometalates and their photoluminescence behavior. *Adv Powder Technol* 24: 549-553.
- 12 Ravichandran K, Saravanakumar K, Chandramohan R, Nandhakumar V (2012) Influence of simultaneous doping of Cd and F on certain physical properties of ZnO nanopowders synthesized via a simple soft chemical route. *Appl. Surf. Sci* 15: 405-410.
- 13 Tarwal NL, Jadhav PR, Vanalakar SA, Kalagi SS, Pawar RC, et al. (2008) Photoluminescence of zinc oxide Nano powder synthesized by a combustion method. *Powder Technol* 20: 185-188.
- 14 Hassan MM, Khan W, Azam A, Naqvi AH (2014) Effect of size reduction on structural and optical properties of ZnO matrix due to successive doping of Fe ions. *J Lumin* 145: 160-166.
- 15 Pookmanee P, Mueangjai M, Phanichphant S, Thanachayanont C (2020) Copper (II) Oxide Powder Prepared by Low Temperature Hydrothermal Method. In: *Key Engineering Materials 2020* 861: 270-276.
- 16 Begum NJ, Ravichandran K (2013) Effect of source material on the transparent conducting properties of sprayed ZnO: Al thin films for solar cell applications. *J Phys Chem Solids* 74: 841-848.
- 17 Ravichandran K, Mohan R, Begum NJ, Swaminathan K, Ravidhas C (2020) Property enhancement of transparent conducting zinc oxide thin films—Effect of simultaneous (Sn+ F) doping. *J Phys Chem Solids* 74: 1794-801.
- 18 Swanboon S, Amorphitoksuk P, Sukolrat A (2011) Influence of a novel triple doping (Ag+Mn+ F) on the magnetic and antibacterial properties of ZnO nanopowders. *Ceram Int* 37: 1359.
- 19 Ravichandran K, Snega S, Begum NJ, Swaminathan K, Sakthivel B (2014) Enhancement in the antibacterial efficiency of ZnO Nano powders by tuning the shape of the Nano grains through fluorine doping. *Superlattice Microst* 69: 17-28.
- 20 Bhadra P, Mitra MK, Das GC, Dey R, Mukherjee S (2011) Interaction of chitosan capped ZnO Nano rods with *Escherichia coli*. *Mater Sci Eng* 31: 929-937.
- 21 Yu J, Li C, Liu S (2008) Effect of PSS on morphology and optical properties of ZnO. *Colloid Interface Sci* 326: 433-438.
- 22 Pan Z, Tian X, Wu S, Yu X, Li Z (2013) Investigation of structural, optical and electronic properties in Al–Sn co-doped ZnO thin films. *Appl Surf Sci* 2: 1.
- 23 He X, Qian H, Zhi Q, Zhang M, Luo J, et al. (2013) Investigation on the enhancement of ultraviolet emission in Ag-ZnO microrods. *Applied surface science*. 283: 571-576.
- 24 Li M, Xu J, Chen X, Zhang X, Wu Y, et al. (2012) Structural and optical properties of cobalt doped ZnO nanocrystals. *Superlattice Microst* 52: 824-33.
- 25 Liu D, Lv Y, Zhang M, Liu Y, Zhu Y, et al. (2014) Defect-related photoluminescence and photocatalytic properties of porous ZnO nanosheets. *J Mater Chem A* 2: 15377-15388.
- 26 Potashnik SJ, Ku KC, Chun SH, Berry JJ, Samarth N, et al. (2001) Effects of annealing time on defect-controlled ferromagnetism in Ga 1– x Mn x As. *Appl Phys Lett* 79: 1495-1497.
- 27 Shah AH, Ahamed MB, Manikandan E, Chandramohan R, Iydrroose M (2013) Magnetic, optical and structural studies on Ag doped ZnO nanoparticles. *J Mater Sci Mater Materials in Electronics*. 24: 2302-2308.

- 28 Sharma A, Singh AP, Thakur P, Brookes NB, Kumar S, et al. (2010) Structural, electronic, and magnetic properties of Co doped SnO₂ nanoparticles. *J Appl Phys* 107: 093-918.
- 29 Sawai J (2003) Quantitative evaluation of antibacterial activities of metallic oxide powders (ZnO, MgO and CaO) by conductimetric assay. *J Microbiol Methods* 54: 177-182.
- 30 Yamamoto O (2001) Influence of particle size on the antibacterial activity of zinc oxide. *J Inorg Mater* 3: 643-646.
- 31 Jones N, Ray B, Ranjit KT, Manna AC(2008) Antibacterial activity of ZnO nanoparticle suspensions on a broad spectrum of microorganisms. *FEMS Microbiol Lett.* 279: 71-76.